Antecedent Drought Condition Affects Responses of Plant Physiology and Growth to Drought and Post-drought Recovery

Ximeng Li[1,2,3]*, Jingting Bao[3,4], Jin Wang[5], Chris Blackman[3] and David Tissue[3]*

[1] College of Life and Environmental Science, Minzu University of China, Beijing, China, [2] Key Laboratory of Ecology and Environment in Minority Areas, Minzu University of China, National Ethnic Affairs Commission, Beijing, China, [3] Hawkesbury Institute for the Environment, Western Sydney University, Penrith, NSW, Australia, [4] School of Life Sciences and Engineering, Lanzhou University of Technology, Lanzhou, China, [5] Shapotou Desert Experiment and Research Station, Cold and Arid Regions Environmental and Engineering Research Institute, Chinese Academy of Sciences, Lanzhou, China

Antecedent environmental conditions may have a substantial impact on plant response to drought and recovery dynamics. Saplings of *Eucalyptus camaldulensis* were exposed to a range of long-term water deficit pre-treatments (antecedent conditions) designed to reduce carbon assimilation to approximately 50 (A_{50}) and 10% (A_{10}) of maximum photosynthesis of well-watered plants (A_{100}). Thereafter, water was withheld from all plants to generate three different levels of water stress before re-watering. Our objective was to assess the role of antecedent water limitations in plant physiology and growth recovery from mild to severe drought stress. Antecedent water limitations led to increased soluble sugar content and depletion of starch in leaves of A_{50} and A_{10} trees, but there was no significant change in total non-structural carbohydrate concentration (NSC; soluble sugar and starch), relative to A_{100} plants. Following re-watering, A_{50} and A_{10} trees exhibited faster recovery of physiological processes (e.g., photosynthesis and stomatal conductance) than A_{100} plants. Nonetheless, trees exposed to the greatest water stress (−5.0 MPa) were slowest to fully recover photosynthesis (A_{max}) and stomatal conductance (g_s). Moreover, post-drought recovery of photosynthesis was primarily limited by g_s, but was facilitated by biochemistry (V_{cmax} and J_{max}). During recovery, slow regrowth rates in A_{50} and A_{10} trees may result from insufficient carbon reserves as well as impaired hydraulic transport induced by the antecedent water limitations, which was dependent on the intensity of drought stress. Therefore, our findings suggest that antecedent water stress conditions, as well as drought severity, are important determinants of physiological recovery following drought release.

Keywords: *Eucalyptus camaldulensis*, drought, non-structural carbohydrate, photosynthesis, stem growth, post-drought recovery

INTRODUCTION

Understanding the impacts of drought stress on plant physiology and growth is essential for predicting the structure and function of plant communities (O'Brien et al., 2017a; Choat et al., 2018; Brodribb et al., 2020), especially within the context of global climate change in which drought episodes are projected to be more common in the future (Dai, 2013). Such impacts, however, can be complex to assess because the consequence of drought stress is a function of resistance and resilience (Stuart-Haëntjens et al., 2018; Li et al., 2020; Schmitt et al., 2020), and both components can be strongly modified by drought events that plants have previously experienced (i.e., antecedent drought) (Kannenberg et al., 2020). Adjustments in plant morphology and/or physiology triggered by antecedent, non-lethal water deficit can often result in divergent responses during subsequent drought stress, with potential impacts on plant performance during recovery (Kannenberg et al., 2020). This is particularly evident in field-grown trees, for which the growth response to recurring drought differs over time (Xu et al., 2010; O'Brien et al., 2017b; Wu et al., 2018; Anderegg et al., 2020). Although the immediate effects of drought stress on plant physiology have been well documented, knowledge gaps still exist on how drought response and post-drought recovery can be modified by antecedent drought conditions (Ruehr et al., 2019).

Leaves are the primary sites of CO_2 and water exchange for the majority of terrestrial plants. How leaves respond to and recover from drought stress can therefore have disproportionately critical effects on plants. Antecedent drought stress can generate multiple adjustments in leaf morphology, physiology, and biochemistry (Gessler et al., 2020). Biological processes related to growth, including cell division and enlargement, are highly sensitive to water stress, and are typically reduced prior to reductions in photosynthesis caused by water deficit (Chapin et al., 1990; Körner, 2015). Consequently, an increase in non-structural carbohydrates (NSCs) is commonly observed in plants subjected to drought stress due to an imbalance in source-sink strength (Sala and Hoch, 2009; Sala et al., 2012; Granda and Camarero, 2017; Piper et al., 2017). Additionally, drought induced variation in tissue NSCs contents may occur in all organs, and the importance of sugar enriched organ to plant performance during water deficit and post-drought recovery can be markedly species-specific (Hagedorn et al., 2016; Joseph et al., 2020; Ouyang et al., 2021). Here, we primarily focus on leaves, the NSCs variation of which have been shown to predominantly regulates plant response to drought stress in some species (Martínez-Vilalta et al., 2016; Signori-Müller et al., 2021)., and dominates the variation of whole plant carbohydrates contents in *Eucalyptus* species (Duan et al., 2013). Depending on its specific type (i.e., soluble sugar and starch), NSCs, together with other secondary metabolites derived from their soluble form, can be involved in physiological processes related to drought resistance such as osmotic regulation, or can be stored as carbon reserves for regrowth upon alleviation of drought stress (Sala et al., 2012; Trifilò et al., 2017; Tomasella et al., 2020). Hence, variation in NSCs induced by antecedent drought conditions can have

important implications for the fate of plants during subsequent drought and recovery cycles.

Of the numerous physiological processes impacted by water limitation, photosynthesis is extensively studied because of its central role in determining plant fitness and sensitivity to water deficit (Flexas et al., 2006a). Leaf photosynthetic rate is co-determined by stomatal conductance and biochemical components of photosynthesis. During drought stress, leaf stomata will partially or completely close to minimize water loss. Given that CO_2 and water molecules share the same pathway at both leaf and cellular levels (e.g., aquaporins), reduced stomatal conductance (g_s) will inevitably constrain photosynthesis (Flexas et al., 2008) and is considered to be the major cause for downregulation of photosynthesis during drought stress (Flexas et al., 2004; Grassi and Magnani, 2005; Zait et al., 2019). On the other hand, the biochemical components of photosynthesis, including the capacity for Rubisco carboxylation (V_{cmax}) and electron transport (J_{max}), are generally less sensitive to dehydration, although a body of literature has shown that both biochemical components can be compromised during drought, and can show similar or even higher drought sensitivity compared to g_s (Zhou et al., 2014). Identifying the key limiting factor for photosynthesis during drought stress and recovery is of utmost importance, especially for modeling vegetation dynamics using ecosystem models. However, acclimation may occur during antecedent drought, thereby generating different physiological responses to subsequent stress conditions (Ruehr et al., 2019; Gessler et al., 2020). Antecedent drought conditions may also alter the relative contribution of each limiting factor during subsequent droughts (Flexas et al., 2009; Menezes-Silva et al., 2017).

The capacity to recover physiological function following the easing of drought stress upon re-watering represents a key dimension of plant drought resilience. However, little is known about the post-drought dynamics and interaction of two fundamental physiological processes, i.e., carbon and water relations (Ruehr et al., 2019). For a given species, the time required for recovery is typically contingent on the severity of drought stress given it determines the extent to which physiological functions are impaired (Flexas et al., 2004; Blackman et al., 2009; Brodribb and Cochard, 2009). With respect to post-drought carbon-relations, it has been shown that stomatal limitation of photosynthesis is prevailing when drought stress is mild or moderate, while biochemical limitation becomes more prominent as drought stress is exacerbated (Flexas et al., 2006a). This is anticipated to result in different recovery dynamics given that reopening of stomata is typically faster than the time it takes to repair photosynthetic machinery after water supply is resumed (Ruehr et al., 2019). Furthermore, rates of photosynthetic recovery from drought are determined by drought severity and its impact on hydraulic function. Recent studies emphasize the pivotal role of water relations in governing plant mortality during drought stress, showing that recovery is no longer possible once the water status has exceeded thresholds of hydraulic impairment due to embolism (Blackman et al., 2009; Brodribb and Cochard, 2009; Choat et al., 2018). Furthermore, plant hydraulics is also intimately coupled with carbon through its impacts on leaf gas

exchange (Brodribb and Holbrook, 2003; Skelton et al., 2017). Thus, assessing the interaction of antecedent drought conditions and drought severity on the recovery dynamics of photosynthesis is crucial for gaining a comprehensive understanding of impacts caused by droughts.

Early experiments studying the influences of drought on plant physiology often subject plants to drought stress differing in either duration (i.e., short or long-term) or severity (i.e., mild to severe), and mainly focused on physiological responses triggered by water limitation (Menezes-Silva et al., 2017). Here, we take a different approach by exposing plants to two drought cycles characterized by different physiological attributes before re-watering and assessing recovery. The first drought was chronic and relatively mild, which was aimed at reducing carbon assimilation and manipulating NSC storage, but not inducing significant impairment in hydraulic function. The second drought was more acute and designed to induce a range of stress levels associated with moderate to severe leaf hydraulic dysfunction. Our aim was to test the potential influences of antecedent drought conditions (i.e., the first drought stress) on the subsequent drought response and eventually the rate of recovery, with particular emphasis on carbon and water relations. We hypothesized that: (1) long-term, mild drought stress will but promote the accumulation of leaf NSC due the hysteresis in ceasing of photosynthesis relative to growth; (2) leaf photosynthesis in plants exposed to antecedent drought conditions will be less affected by subsequent drought than control plants; (3) both stomatal and non-stomatal limitations will restrict the rate of recovery of photosynthesis following re-watering; and (4) the time required for regaining physiological function is dependent on the severity of the drought.

MATERIALS AND METHODS

Plant Material and Experimental Design

Eucalyptus camaldulensis, commonly known as river red gum, is one of the most widely distributed tree species across Australia. *E. camaldulensis* can adapt to diverse climatic conditions, ranging from tropical to temperate ecosystems. At the local scale, the distribution of *E. camaldulensis* is primarily confined to locations where soil water availability is ample, such as riverbanks or floodplains, where it often appears as the dominant species, providing significant ecological functional services (Butcher et al., 2009; Doody et al., 2015).

Seeds of river red gum (*E. camaldulensis* subsp. *camaldulensis*) were obtained from the Australian Tree Seed Centre (Canberra, ACT) and germinated in forestry tubes placed in a sunlit poly-tunnel provided by Greening Australia (Richmond, NSW, Australia) for 2 months. On October 20, 2017, 40 similarly sized seedlings (approximately 15 cm tall) were transplanted into 15 × 40 cm (diameter × height) cylindrical pots filled with *ca.* 9 kg of moderately fertile sandy loam soil. Twenty pots were randomly selected and placed in one of the two adjacent naturally sunlit glasshouse bays located at the Hawkesbury Campus, Western Sydney

University, Richmond, NSW Australia. Environmental conditions within both glasshouse bays were controlled, with temperature set to 26/18°C (day/night), which represents the local average air temperature during the growing season, and air CO_2 concentration set to 400 µmol mol^{-1}. This environmental condition was maintained throughout the experimental period. All seedlings were irrigated daily and fed with slow-release fertilizer biweekly (Osmocote, All-Purpose, Scotts, Australia) to ensure the absence of water and nutrient limitations.

Starting on November 28, 2017, 30 plants with similar height and basal diameter (75 cm and 0. 5 cm, respectively) were selected for the experiment. Plants were evenly divided into three groups, so that we could apply three levels of drought in the first round of drought treatment (i.e., antecedent drought condition). Levels of antecedent drought conditions were defined based on the photosynthetic rate measured under saturating light and ambient air CO_2 conditions (A_{max}), with A_{max} of stressed plants maintained at approximately 50 (A_{50}) and 10% (A_{10}) relative to that of the well-watered plants (A_{100}). For A_{50} and A_{10} plants, drought stress was imposed by withholding irrigation. Leaf A_{max} was monitored daily for each individual until the desired values were achieved. Pots were labeled and weighed immediately. During the period of antecedent drought treatment, pot-specific soil water content was maintained by weighing individual pots daily in the morning and replacing the water loss from the previous day. Leaf gas exchange was measured every 1–3 days during the same period to ensure that the targeted A_{max} could be maintained. It has been shown that complete stomatal closure in *E. camaldulensis* typically occurs when leaf water potential reaches approximately −1.5 MPa (Zhou et al., 2014), which is less negative than the water potential threshold for the incipient hydraulic dysfunction (see below). Given that the stomata remained open during the phase of antecedent drought treatment, no hydraulic impairment was likely incurred by the intensity of drought stress.

After 48 days of antecedent drought treatment, plants in each drought treatment group were further divided into three sub-groups to implement the second round of drought treatment, so that each sub-group contained 3–4 individuals. The second drought treatment aimed to generate dysfunction in water transport and was therefore applied based on previously determined hydraulic vulnerability curves of leaves. Hence, irrigation water was withheld until midday leaf water potential (Ψ_{leaf}) reached *ca.* −3.5, −4.5, or −5.0 MPa for the three drought groups; these values corresponded to the Ψ_{leaf} at which 12, 50, and 88% loss of leaf hydraulic conductivity (K_{Leaf}) occurred in this species (Blackman et al., unpublished data). For each individual, Ψ_{Leaf} was measured once daily. In the controlled environment of the glasshouse bays, the target Ψ_{Leaf} was typically achieved in 1–3 days. Once the targeted Ψ_{leaf} was attained, photosynthetic CO_2 response (AC_i) curves were measured; thereafter, the pot was re-watered to field capacity to alleviate the water stress and allow for recovery. Physiological measurements, including Ψ_{Leaf} and AC_i curves were repeated on 3, 7 and 14 days following re-watering during the recovery phase to assess the degree of physiological recovery over time.
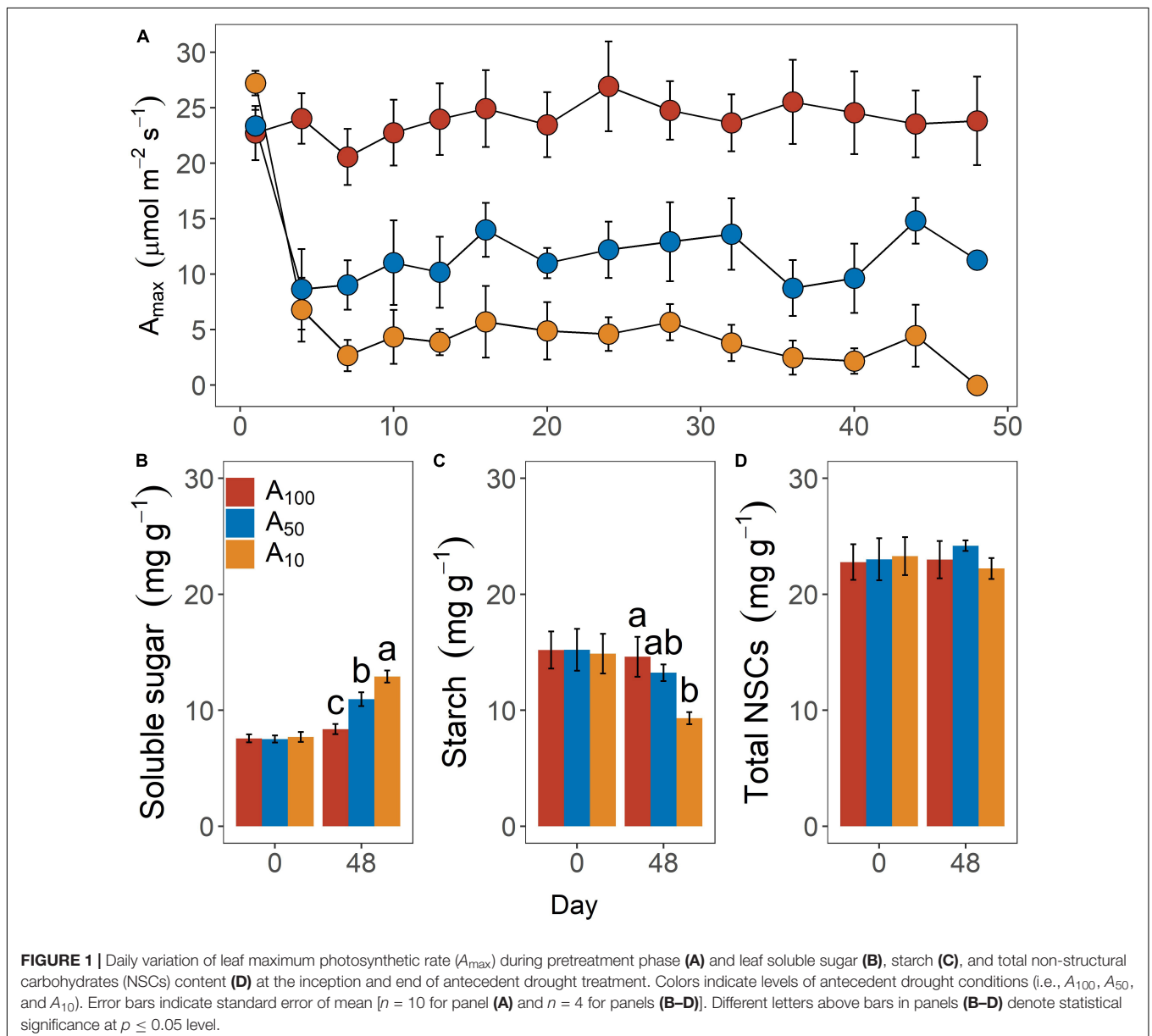
Gas Exchange Measurements

Leaf gas exchange measurements, including A_{max}, stomatal conductance (g_s), and AC_i curves were measured between 9 am and noon with up to four cross-calibrated open gas exchange systems (LI-6400XT, Li-Cor, Lincoln, NE, United States) equipped with red-blue LED light sources (6400-02B) and an external CO_2 injector (6400-01). For each individual plant, one upper canopy, fully expanded leaf was tagged and consistently used for gas exchange measurements throughout the experiment. For spot measurements, gas exchange variables including A_{max} and g_s were recorded under saturating light (i.e., 1,500 μmol m^{-2} s^{-1}). Cuvette CO_2 concentration and temperature were set to match the ambient conditions (i.e., 400 μmol mol^{-1} and 26°C, respectively). Leaf AC_i curves were generated by recording A_{max} under varying cuvette CO_2 concentrations: 400,

300, 200, 100, 400, 600, 800, 1,000, and 1,200 μmol mol^{-1}, with other environmental parameters identical to the spot measurements. Before each measurement, leaves were allowed to acclimate in the cuvette for up to 20 min and data were recorded after the readings were stable. During all gas exchange measurements, relative humidity and leaf-to-air water vapor deficit in the cuvette typically varied between 50 and 60% and 1.5–2.0 kPa, respectively.

Leaf Non-structural Carbohydrate Concentrations

Leaf carbohydrate content was assessed at the beginning and the end of the antecedent drought stress phase. Within each antecedent drought treatment group, 2–4 upper canopy

FIGURE 1 | Daily variation of leaf maximum photosynthetic rate (A_{max}) during pretreatment phase **(A)** and leaf soluble sugar **(B)**, starch **(C)**, and total non-structural carbohydrates (NSCs) content **(D)** at the inception and end of antecedent drought treatment. Colors indicate levels of antecedent drought conditions (i.e., A_{100}, A_{50}, and A_{10}). Error bars indicate standard error of mean [$n = 10$ for panel **(A)** and $n = 4$ for panels **(B–D)**]. Different letters above bars in panels **(B–D)** denote statistical significance at $p \leq 0.05$ level.

leaves were collected for each plant from 4 randomly selected individuals. The leaf samples were immediately oven-dried at 80°C for 24 h to stop metabolism and then stored in −20°C freezer until measurement. Leaf starch and soluble sugars concentrations were determined following the protocol described by Duan et al. (2013). Concisely, dried materials were grounded to a fine powder in a ball mill, and then weighed for 20 mg. Samples were extracted with 80% aqueous ethanol, then boiled at 95°C for 30 min and centrifuged at 3,000 rpm for 5 min. Supernatant was collected, re-extracted with ethanol and water, and then subjected to the procedures described above. The final supernatant was reserved and evaporated at 40°C using a rotational vacuum concentrator (RVC 2-25 CD, Christ, Germany). Starch content (mg g^{-1}) was determined from the remaining pellets after extraction and assayed with a total starch assay kit (Megazyme International Ireland Ltd., Wicklow, Ireland). Total soluble sugar content (mg g^{-1}) was measured from the supernatants by the anthrone method. Total NSCs content (mg g^{-1}) was calculated as the sum of soluble sugar and starch.

Growth Measurements

To minimize canopy leaf loss, leaf samples used for Ψ_{Leaf} determination were measured for leaf area using leaf area meter (LI-3100, Li-Cor, Lincoln, NE, United States). Samples were then oven-dried for at least 72 h to constant mass, and leaf mass per area (LMA, g m^{-2}) was calculated as the ratio of dry mass to leaf area.

Plant height (H, cm) and basal diameter (D, mm) were measured biweekly throughout the experimental period. Basal diameter was measured using digital calipers at *ca.* 3 cm above soil level, while plant height was considered as the distance from the soil level to the apex of the main stem. Stem volume was estimated as H × D^2 (cm^3), and stem volume index growth rate (VIGR, cm^3 day^{-1}) was calculated as the increment of stem volume between measurement periods divided by the number of days.

Data Analysis

Leaf AC$_i$ curve data were fitted to the FvCB model using *fitaci* function of the Plantecophys R Package to estimate the maximum carboxylation rate of Rubisco (V_{cmax}, μmol m^{-2} s^{-1}) and electron transport rate (J_{max}, μmol m^{-2} s^{-1}) (Duursma, 2015). The speed of recovery is assessed by calculating the time required for specific physiological variables to regain 50% of its maximum ($t_{1/2}$, day), according to Brodribb and Cochard (2009). In short, the percentage of recovery relative to its maximum, measured from each individual within the same treatment group, was pooled together and was plotted against the corresponding number of days. The relationship was fitted using a linear regression and $t_{1/2}$ was then extrapolated from the linear function. The estimation of $t_{1/2}$ was limited to A_{max} and g_s given that the reduction in other physiological variables never surpassed 50% of their maximum.

Leaf NSCs, including the content of soluble sugar, starch and total NSCs content at the end of antecedent drought treatment, were analyzed using one-way ANOVA to test the difference among treatment groups. Physiological data including the A_{max},

g_s, V_{cmax}, and J_{max} measured during the recovery phase were presented as the percentage relative to their corresponding values measured prior to the implementation of the antecedent drought treatment. All time-series data were analyzed using the one-way repeated measurement ANOVA with the *ezANVOA* function in the ezANVOA package, with the levels of drought treatment and time of measurement considered as between- and within-subject factors, respectively. In addition, within each measurement time point, one-way ANOVA was used to test the difference among antecedent drought treatment groups. Following all one-way ANOVA, Tukey's HSD *post hoc* was applied using the *HSD.test* function in the agricolae package for comparison among means. All data were tested for normality and homogeneity of variance before statistical analysis was performed. Statistically significant differences were considered when $p \leq 0.05$. Data process and analysis were performed under R 3.5.3 statistical computing environment (R Core Team, 2013).

RESULTS

Effects of Antecedent Drought Conditions on Leaf Photosynthesis, Carbohydrate Content, and Growth

Leaf photosynthetic rate under saturating light (A_{max}, μmol m^{-2} s^{-1}) differed significantly across levels of antecedent drought conditions (**Figure 1A**; $p < 0.01$). Consistent with our objective, A_{max} in drought-stressed plants (i.e., A_{50} and A_{10}) was constantly maintained at the desired levels during the period of antecedent drought treatment. Interaction between time and drought treatment was observed, but only limited to the first day of measurement, with A_{max} of A_{10} being slightly higher (*ca.* 4.0 μmol m^{-2} s^{-1}) than that of A_{100} and A_{50}.

Contents of leaf NSCs, including soluble sugar (**Figure 1B**), starch (**Figure 1C**), and total NSCs (**Figure 1D**) did not differ across groups before drought treatments were applied. Differences in these variables were observed after 48 days of water restriction during the antecedent treatment. Soluble sugar of A_{10} (12.9 ± 0.5 mg g^{-1}) and A_{50} (10.9 ± 0.6 mg g^{-1}) plants were significantly higher than that of A_{100} plants (8.4 ± 0.4 mg g^{-1}; $p = 0.02$). Starch content also differed significantly across groups but exhibited an inverse pattern ($p = 0.03$), with starch content being 9.3 ± 0.5 mg g^{-1}, 13.2 ± 0.7 mg g^{-1} and 14.6. ± 1.7 mg g^{-1} for A_{10}, A_{50}, and A_{100} plants. Growth rate was strongly impeded by drought treatment ($p < 0.01$; data not shown). The volume index growth rates (VIGR, cm^3 day^{-1}) were 5.23 ± 0.31 cm^3 day^{-1}, 0.99 ± 0.11 cm^3 day^{-1} and 0.39 ± 0.07 cm^3 day^{-1} for A_{100}, A_{50}, and A_{10} plants, respectively.

Responses of Leaf Photosynthesis and Water Relations to Subsequent Drought Stress

All physiological variables, including A_{max}, light saturated stomatal conductance (g_{smax}, mol m^{-2} s^{-1}), carboxylation rate of Rubisco (V_{cmax}, μmol m^{-2} s^{-1}) and electron transport rate (J_{max}, μmol m^{-2} s^{-1}) were significantly decreased by

subsequent drought stress (**Figure 2** and **Table 1**; day 0). In general, the percentage loss of function from maximum values for each physiological parameter, increased with drought severity; however, there was an exception in V_{cmax} and J_{max}, where the relative values for plants at −4.5 MPa were 25.4 and 15.4% higher, respectively, than plants at −3.5 MPa. All physiological variables in plants subjected to antecedent drought conditions, and subsequently to variable drought stress, were less affected compared with control plants that were well-watered and did not experience an antecedent drought stress (**Figure 2**).

Recovery Dynamics of Leaf Photosynthesis, Water Relations, and Plant Growth After Re-watering

Recovery in photosynthetic variables was dependent on the degree of antecedent water deficit and drought severity (**Figures 2**, **3** and **Table 1**). For A_{max} and associated components (i.e., g_s, V_{cmax} and J_{max}), A_{50} and A_{10} plants consistently showed faster rates of recovery compared to A_{100} plants; these effects were stronger as the intensity of subsequent drought stress increased. For example, for plants at −4.5 MPa, A_{max}, V_{cmax} and J_{max} attained nearly or complete recovery on the third day of re-watering, whereas full recovery of these variables in A_{100} plants was much slower; e.g., A_{max} and J_{max} did not reach the values
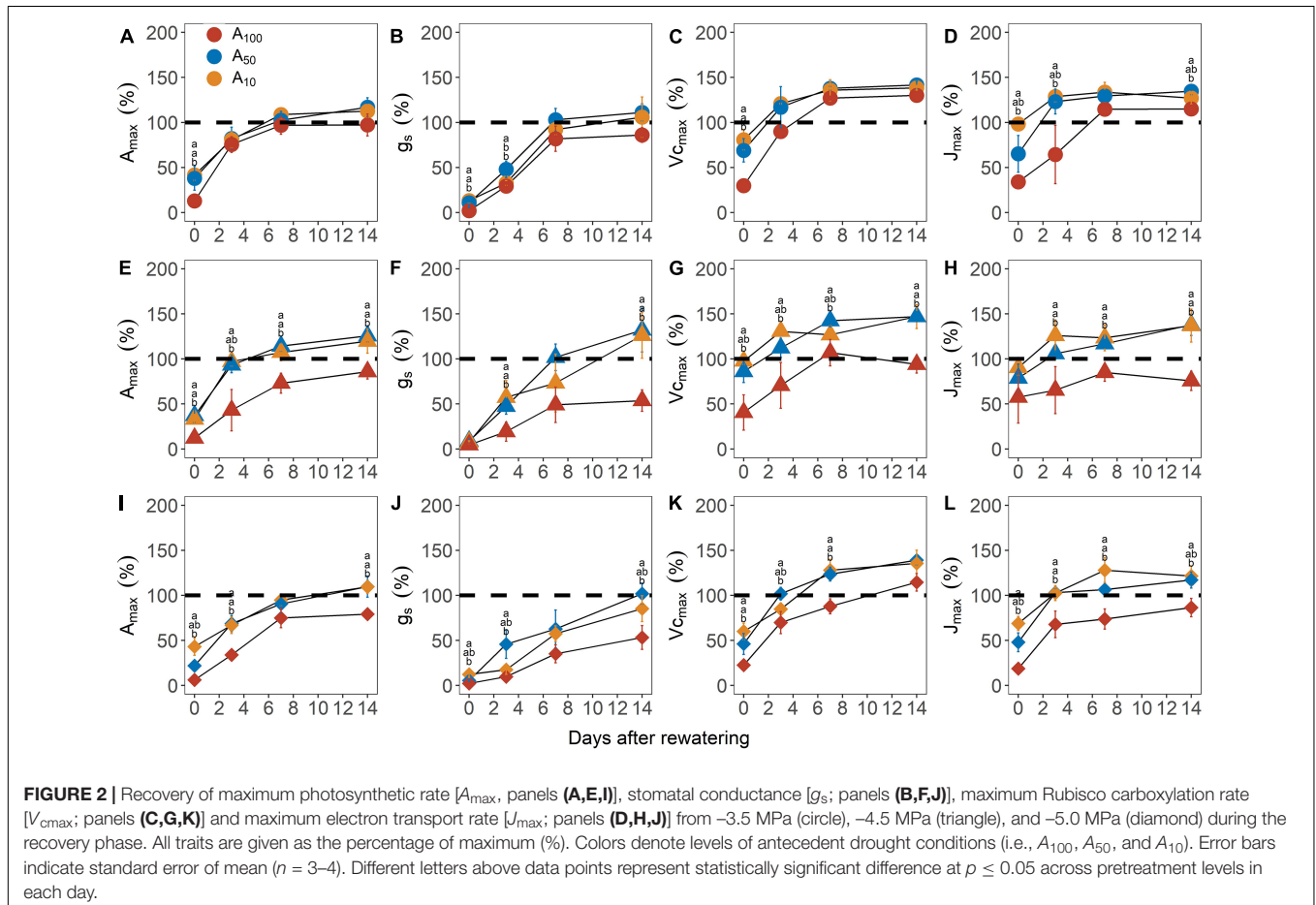
measured before the implementation of the antecedent drought treatments even after 14 days of re-watering (**Figures 2E,G,H**). Notably, for V_{cmax} and J_{max}, the values during the recovery phase were up to 50% higher than their pre-stress levels, suggesting a compensatory response to the previous drought stress.

Upon re-watering, leaf water potential (Ψ_{Leaf}, −MPa) recovered rapidly, reaching pre-stress values within 3 days in most plants, regardless of antecedent and subsequent drought treatment (**Figure 4**). Across drought treatment, Ψ_{Leaf} of plants exposed to antecedent drought was generally less negative than that of control plants, although the difference was not significant.

Upon re-watering and release of the drought stress, all plants showed stem regrowth, but with differing rates of growth. For plants dried to −3.5 and −4.5 MPa, VIGR of A_{100} plants was significantly higher than that of A_{50} and A_{10} plants (**Table 2**; $p < 0.05$ in both cases), while VIGR did not vary across levels of antecedent drought treatment when exposed to severe water stress ($p = 0.17$).

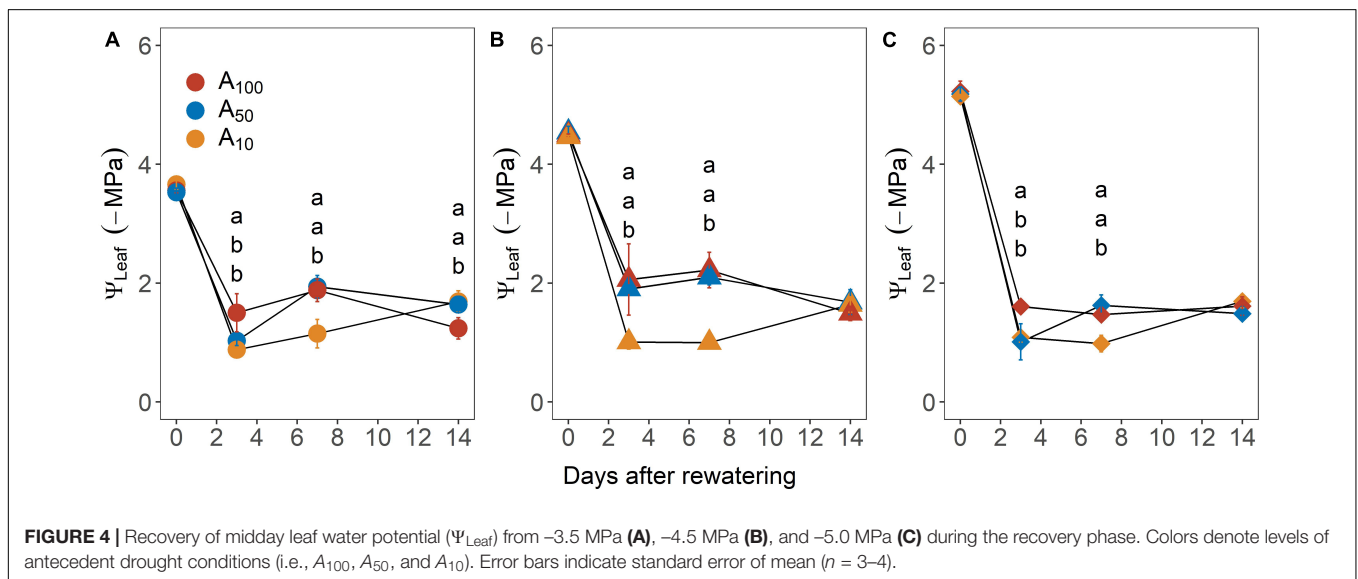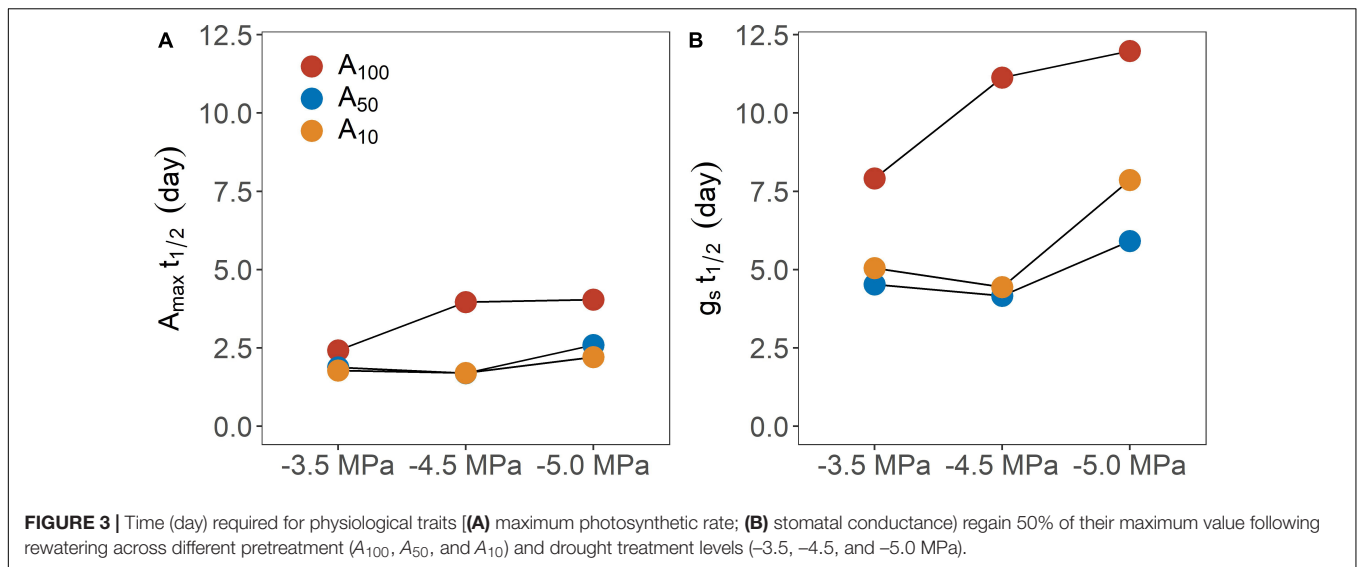## The Relationships Between Recovery of Leaf Photosynthesis and Associated Physiological Variables

Recovery of leaf carbon assimilation was closely related to variables associated with CO_2 diffusion and biochemistry

FIGURE 2 | Recovery of maximum photosynthetic rate [A_{max}, panels **(A,E,I)**], stomatal conductance [g_s; panels **(B,F,J)**], maximum Rubisco carboxylation rate [V_{cmax}; panels **(C,G,K)**] and maximum electron transport rate [J_{max}; panels **(D,H,J)**] from –3.5 MPa (circle), –4.5 MPa (triangle), and –5.0 MPa (diamond) during the recovery phase. All traits are given as the percentage of maximum (%). Colors denote levels of antecedent drought conditions (i.e., A_{100}, A_{50}, and A_{10}). Error bars indicate standard error of mean (n = 3–4). Different letters above data points represent statistically significant difference at $p \leq 0.05$ across pretreatment levels in each day.

TABLE 1 | Statistical analysis for the difference in the percentage of recovery in maximum photosynthetic rate (A_{max}), stomatal conductance (g_s), maximum carboxylation rate of Rubisco (V_{cmax}), maximum electron transport rate (J_{max}), and midday leaf water potential (Ψ_{Leaf}) across different drought treatments (i.e., −3.5, −4.5, and −5.0 MPa) during the phase of recovery (i.e., day 0, 3, 7, and 14).

Traits	Treatment (MPa)	Days of recovery										
		Day 0			Day 3			Day 7			Day 14		
		SS	*F*-value	*p*	SS	*F*-value	*p*	SS	*F*-value	*p*	SS	*F*-value	*p*
A_{max}	−3.5	1,480.42	$8.28_{[2,6]}$	0.02	74.60	$0.36_{[2,6]}$	0.71	213.61	$1.50_{[2,6]}$	0.30	647.07	$3.16_{[2,6]}$	0.12
	−4.5	1,085.27	$14.16_{[2,7]}$	<0.01	5,444.10	$13.00_{[2,7]}$	<0.01	2,926.70	$18.34_{[2,7]}$	<0.01	2,761.74	$14.25_{[2,7]}$	<0.01
	−5.0	2,051.82	$24.57_{[2,6]}$	<0.01	2,286.50	$17.75_{[2,6]}$	<0.01	660.54	$3.93_{[2,6]}$	0.08	1,843.29	$12.21_{[2,6]}$	<0.01
g_s	−3.5	206.62	$8.49_{[2,6]}$	0.02	590.78	$7.75_{[2,6]}$	0.02	666.74	$2.57_{[2,6]}$	0.16	1,051.10	$2.39_{[2,6]}$	0.17
	−4.5	28.31	$4.17_{[2,7]}$	0.07	2,338.60	$6.56_{[2,7]}$	0.03	4,182.90	$3.84_{[2,7]}$	0.08	11,410.70	$12.40_{[2,7]}$	<0.01
	−5.0	156.82	$17.52_{[2,6]}$	<0.01	2,154.52	$11.63_{[2,6]}$	<0.01	1,290.70	$3.15_{[2,6]}$	0.12	3,678.90	$10.63_{[2,6]}$	0.01
V_{cmax}	−3.5	4,267.40	$18.86_{[2,6]}$	<0.01	1,691.20	$4.88_{[2,6]}$	0.06	197.81	$2.06_{[2,6]}$	0.21	215.01	$3.83_{[2,6]}$	0.32
	−4.5	5,461.40	$14.96_{[2,7]}$	<0.01	5,689.90	$11.17_{[2,6]}$	<0.01	1,903.70	$10.20_{[2,7]}$	0.01	5,620.60	$28.28_{[2,7]}$	<0.001
	−5.0	2,148.16	$13.75_{[2,6]}$	<0.01	1,543.22	$9.49_{[2,6]}$	0.01	2,906.22	$16.11_{[2,6]}$	<0.01	1,064.80	$4.77_{[2,6]}$	0.06
J_{max}	−3.5	6,181.50	$19.36_{[2,6]}$	<0.01	7,646.80	$9.03_{[2,6]}$	0.02	599.52	$4.34_{[2,6]}$	0.07	588.69	$10.65_{[2,6]}$	0.01
	−4.5	1,678.40	$1,678.40_{[2,6]}$	0.19	5,729.80	$8.66_{[2,7]}$	0.02	2,536.37	$11.80_{[2,7]}$	<0.01	7,610.30	$19.41_{[2,6]}$	<0.01
	−5.0	3,821.10	$31.14_{[2,6]}$	<0.001	2,457.65	$12.08_{[2,6]}$	<0.01	4,486.60	$19.31_{[2,6]}$	<0.01	2,183.80	$10.77_{[2,6]}$	0.01
Ψ_{leaf}	−3.5	0.03	$3.23_{[2,6]}$	0.11	0.63	$8.58_{[2,6]}$	0.02	1.16	$13.41_{[2,6]}$	<0.01	0.37	$6.49_{[2,6]}$	0.03
	−4.5	0.01	$1.36_{[2,6]}$	0.33	1.92	$7.59_{[2,6]}$	0.02	2.71	$36.83_{[2,6]}$	<0.001	0.06	$1.20_{[2,6]}$	0.37
	−5.0	0.01	$0.36_{[2,6]}$	0.71	0.63	$9.35_{[2,6]}$	0.01	0.68	$20.40_{[2,6]}$	<0.01	0.07	$2.45_{[2,6]}$	0.17

Presented statistical outcomes including sum of squares (SS), F-value, and calculated value of probability (p). Subscripted numbers following the F values indicate degrees of freedom for between and within group factors. Post hoc analysis was applied when p ≤ 0.05 with the resulting being reported in **Figure 2**.

FIGURE 3 | Time (day) required for physiological traits [**(A)** maximum photosynthetic rate; **(B)** stomatal conductance) regain 50% of their maximum value following rewatering across different pretreatment (A_{100}, A_{50}, and A_{10}) and drought treatment levels (–3.5, –4.5, and –5.0 MPa).

FIGURE 4 | Recovery of midday leaf water potential (Ψ_{Leaf}) from –3.5 MPa **(A)**, –4.5 MPa **(B)**, and –5.0 MPa **(C)** during the recovery phase. Colors denote levels of antecedent drought conditions (i.e., A_{100}, A_{50}, and A_{10}). Error bars indicate standard error of mean (n = 3–4).

TABLE 2 | Volume index growth rates (cm^3 day^{-1}; VIGR) of plants across all drought treatments during the recovery phase.

Pre-treatment	Drought treatment		
	−3.5 MPa	**−4.5 MPa**	**−5.0 MPa**
A_{100}	6.63 ± 0.85^a	5.10 ± 0.69^a	3.21 ± 0.08^a
A_{50}	3.36 ± 0.47^b	3.91 ± 0.42^{ab}	3.21 ± 0.38^a
A_{10}	3.24 ± 0.37^b	2.97 ± 0.50^b	3.58 ± 0.24^a

Data are shown as mean ± standard deviation of mean (n = 3–4). Superscripts indicate significant difference at p ≤ 0.05 level within each drought treatment group.

(**Figure 5**). When data were pooled together, a curvi-linear relationship was found between the percentage recovery of A_{max} and g_s. These two variables were linearly related up to 70% recovery of A_{max}, with a slope of 1.38. In addition, recovery of A_{max} was also linearly related to V_{cmax} (r^2 = 0.91, p < 0.001) and

J_{max} (r^2 = 0.77, p < 0.001), with the slope of the linear regression being 0.94 and 0.97, respectively.

DISCUSSION

We applied different levels of drought stress and measured plant carbohydrates, gas exchange, plant water status and growth, to investigate the influences of antecedent drought conditions on the response of plants during subsequent drought stress and recovery dynamics. Although photosynthesis, growth and the form of leaf carbohydrate varied across different levels of antecedent drought treatment, total NSC content did not vary. During subsequent drought stress, plants that experienced antecedent drought conditions (i.e., A_{50} and A_{10}) were less affected compared with the control (i.e., A_{100}) in terms of carbon assimilation, maximum rate of Rubisco carboxylation and
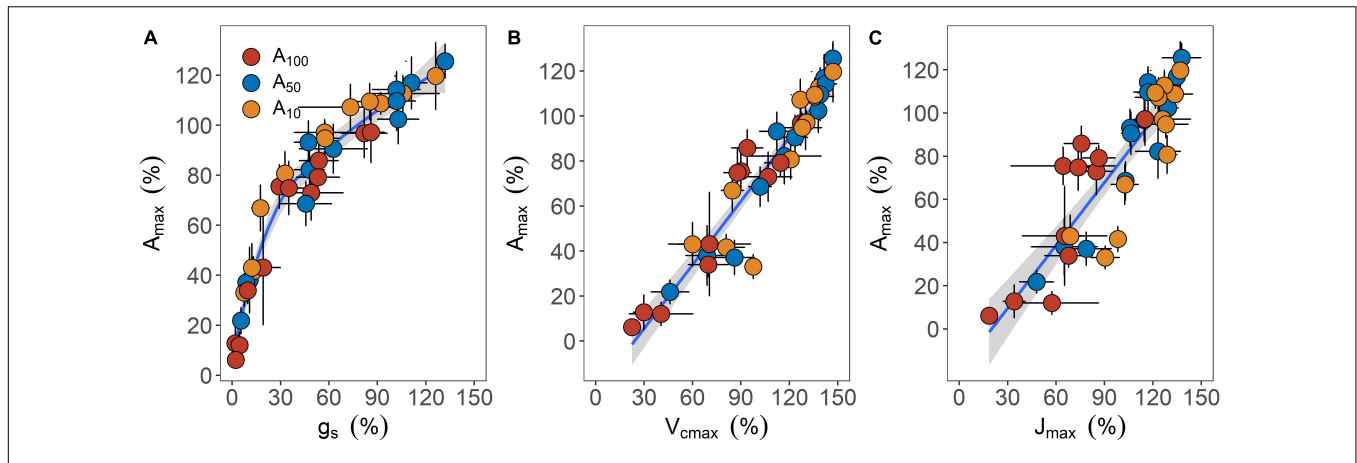
FIGURE 5 | The relationships between maximum photosynthetic rate (A_{max}) and stomatal conductance [g_s, panel **(A)**], maximum carboxylation rate of Rubisco [V_{cmax}, panel **(B)**] and maximum electron transport rate **(C)** during the recovery phase. All traits are expressed as the percentage of maximum relative to the values before drought treatment was applied. Error bars indicate standard error of mean (n = 3–4). Data are pooled across all drought treatment groups and are fitted with nonlinear [**(A)** y = 28.86 ln(x) − 25.57, R^2 = 0.95] or linear regressions [**(B)** y = 0.94x − 22.74, R^2 = 0.91; and **(C)** y = 0.97x − 19.46, R^2 = 0.78] when possible. Shaded regions surrounding fitted lines represent 95% confident interval.

electron transport. Post-drought recovery of leaf photosynthesis was controlled by both stomatal and non-stomatal limitation. Importantly, time to recovery was dependent on both antecedent drought conditions and the severity of subsequent drought stress, with faster physiological recovery in antecedent plants compared to controls observed only when plants had been exposed to the more severe drought treatment. Overall, we found that antecedent drought conditions altered the response of leaf carbon assimilation to ensuing water limitation and resumption in *E. camaldulensis*, suggesting that both drought resistance and resilience are dependent on the exposure of plants to historical drought events.

Variation of Leaf Carbohydrate Content During Sustained Drought

Greater reductions in growth relative to photosynthesis will theoretically lead to carbohydrate accumulation (Chapin et al., 1990; Sala et al., 2012; Piper et al., 2017). However, experimental evidence regarding the impact of drought on leaf carbohydrate content is inconsistent (Klein et al., 2014; Martínez-Vilalta et al., 2016; Chuste et al., 2020; He et al., 2020). For example, leaves of *Eucalyptus saligna* seedlings exposed to drought exhibited higher NSC content compared to well-watered controls (Ayub et al., 2011), whereas an opposite pattern was observed in leaves of *Eucalyptus globulus* and *Eucalyptus smithii* (Duan et al., 2013; Mitchell et al., 2013). In the present study, growth nearly ceased while leaf photosynthesis continued during the phase of antecedent drought treatment, yet total NSC content remained stable across treatment groups (**Figure 1**), similar to the findings reported by Klein et al. (2014) in branches of *Pinus halepensis* subjected to drought. The lack of change in NSC content during drought may emerge due to several reasons. Firstly, the total NSC content can vary markedly among organs (He et al., 2020); therefore, the NSC content of a single organ does not comprehensively reflect drought-induced changes

in whole plant carbon reserve, although it can be driven by one organ (e.g., Duan et al., 2013). Secondly, the carbohydrate content may be influenced by the duration of drought exposure. For example, initially accumulated carbohydrate due to growth cessation may be depleted due to increased rates of other carbon-consuming metabolic processes such as respiration or synthesis of compatible osmolytes, as drought stress proceeds (Flexas et al., 2005; Tomasella et al., 2020).

Although total NSC content was not affected by drought, the relative contribution of soluble sugar and starch content to NSC was consistent with the findings of earlier studies (He et al., 2020). It has been shown that the depolymerization of starch into soluble sugar during drought stress will facilitate osmotic regulation, thereby lowering the risk of hydraulic impairment by increasing water acquisition (Trifilò et al., 2017; Tomasella et al., 2020). The concomitant increase in soluble sugar and decrease in starch, therefore reflects the shift in the functionality of carbohydrate from growth to maintenance, in which starch primarily acts as carbon reserve while soluble sugar performs immediate metabolic functions (Martínez-Vilalta et al., 2016).

Antecedent Drought Condition Promotes Drought Resistance of Photosynthesis

Our second hypothesis was partially supported by the observation that leaf A_{max} was generally higher in plants exposed to antecedent drought conditions, and then exposed to subsequent drought. The smaller reduction in A_{max} was attributed to the biochemical components of photosynthesis rather than gas exchange, as g_s did not differ across levels of drought stress in plants exposed to antecedent drought (**Figure 2**). On the other hand, biochemical components of photosynthesis can also acclimate to drought. With respect to Rubisco carboxylation, it has been reported that water limitation, although uncommon, can increase the catalytic efficiency of Rubisco by increasing either the amount of enzyme or activation

state (Galmés et al., 2013; Menezes-Silva et al., 2017). Likewise, in some species, an increased electron transport rate has been found in leaves exposed to drought (Kitao et al., 2003), although the functional significance of the adjustment is unclear, given that photosynthesis is rarely limited by RuBP regeneration under drought stress.

Recovery Is Co-limited by Stomatal and Non-stomatal Limitation

The decreased g_s, V_{cmax}, and J_{max} relative to their pre-stress values, in conjunction with the correlations between the percentage recovery of A_{max} and these components, indicate stomatal and non-stomatal limitation of photosynthesis during both drought stress and post-drought recovery phase (**Figure 2**). Noticeably, after the resumption of irrigation, although the recovery of A_{max} was associated with recovery of both g_s and biochemical components, the slope of the $A_{max} - g_s$ relationship was much steeper than the slope of the $A_{max} - V_{cmax}$ or $A_{max} - J_{max}$ relationship, up to *ca.* 70% of full recovery (**Figure 5**); hence, the initial phase and major fraction of the full recovery of A_{max} was primarily driven by the restoration of g_s. It has been suggested that drought induced down-regulation of leaf photosynthesis is mainly attributed to diffusive limitation rather than biochemical limitation (Flexas et al., 2004, 2006b). However, down-regulation of photosynthesis due to decreased V_{cmax} caused by inactivation of Rubisco and RuBP content have been reported in a number of species (Parry et al., 2002; Carmo-Silva et al., 2010; Galmés et al., 2013). It is likely that the occurrence of biochemical limitation depends on the strength of water limitation. For instance, decreased V_{cmax} or J_{max} only emerged when drought stress was severe and g_s approached very low values, approximately 20% of the control (Flexas et al., 2004), suggesting that decreased biochemical efficiency of photosynthesis may have limited the recovery of photosynthesis as the highest g_s accounted for *ca.* 14% of the pre-stressed value even for plants subjected to the mildest drought stress (i.e., −3.5 MPa). Nonetheless, it could be argued that decreased biochemical function could be an artifact due to drought-induced reduction in mesophyll conductance (g_m). Indeed, V_{cmax} remains unaffected by water stress when the resistance of g_m to CO_2 diffusion is accounted for when calculating Rubisco carboxylation rate from response curves (Flexas et al., 2006a, 2008). However, by accounting for g_m, Zhou et al. (2014) found that both diffusive and biochemical limitation can contribute to down-regulation of photosynthesis during drought in a wide range of species, including *E. camaldulensis*; e.g., V_{cmax} can decrease by 50% at −2.0 MPa, regardless of the variation in the value of g_m under drought. Still, further work is clearly needed to confirm our observation by assessing the potential effects of g_m on the measurement of biochemical components of photosynthesis, using plants subjected to the same drought treatment.

Recovery From Drought Depends on Antecedent Condition and Severity

Shorter $T_{1/2}$ for A_{max} and g_s was found in seedlings exposed to antecedent drought conditions, which apparently generated drought-induced acclimation of photosynthesis, although the

difference in $T_{1/2}$ for A_{max} at −3.5 MPa was less pronounced between well-watered control and plants exposed to antecedent drought treatment. Notably, A_{10} and A_{50} plants exhibited similar $t_{1/2}$ for both A_{max} and g_s at less negative water potentials (i.e., −3.5 and −4.5 MPa), while the time for recovery diverged at −5.0 MPa. Hence, increasing the level of antecedent drought conditions would not consistently confer rapid recovery, especially when subsequent drought stress was severe (**Figure 4**), suggesting an interaction between the intensity of consecutive drought conditions. Overall, trees exposed to more severe drought stress typically need longer $T_{1/2}$. This finding is consistent with early studies showing that the time required for recovery is dependent on the severity of drought stress (Blackman et al., 2009; Brodribb and Cochard, 2009). Given that the subsequent drought stress was designed to reduce K_{Leaf}, a mechanistic explanation bridging the time to recovery and drought severity may be the following: that the greater the impairment of K_{Leaf}, the longer it would take A_{max} and g_s to fully recover, thereby delaying whole plant recovery. Of note, two implicit assumptions behind this interpretation are: (a) recovery of leaf photosynthesis is driven by the alleviation of stomatal limitation; and (b) the recovery dynamics of g_s are primarily governed by the recovery in K_{Leaf}. As has been discussed above, stomatal limitation played a major role in limiting the recovery of photosynthesis during the recovery phase. On the other hand, it is known that the stomatal openness highly depends on leaf water status, which is a function of K_{Leaf} at a given stem-to-leaf water potential gradient. In support, the variation of K_{Leaf} has been found to synchronize with that of g_s at diurnal scales (Brodribb and Holbrook, 2004) and the restoration of leaf gas exchange has been facilitated by the recovery of K_{Leaf} following drought stress (Galmés et al., 2007; Skelton et al., 2017). In the current study, the recovery of g_s was slower as drought stress and in turn hydraulic impairments intensified, which is consistent with the established theory linking plant hydraulics and gas exchange.

CONCLUSION

Our findings demonstrate that antecedent drought conditions may modify leaf biochemistry and physiology, which can be translated into different responses upon subsequent drought stress and recovery dynamics, following the alleviation of water limitation. Antecedent drought triggered an increase in soluble sugar content, which may have facilitated the recovery of water status by osmotic regulation and the maintenance of hydraulic integrity by lowering the vulnerability to embolism (De Baerdemaeker et al., 2017). The recovery of carbon assimilation was ultimately limited by decreased gas exchange capacity because of hydraulic impairment, which depended on the severity of the subsequent drought. Growth following re-watering was limited by the lack of carbon reserves, thus highlighting the importance of plant hydraulics and carbohydrates in regulating plant drought resistance and resilience. Overall, the response of plants to drought stress appears to be a function of the antecedent conditions and the subsequent drought, which should be considered in combination when assessing the response of plants to drought.

DATA AVAILABILITY STATEMENT

The raw data supporting the conclusions of this article will be made available by the authors, without undue reservation.

AUTHOR CONTRIBUTIONS

DT and CB conceived and designed the research and revised the manuscript. JW and JB conducted the experiments. XL analyzed the data and wrote the early draft of the manuscript. All authors read and approved the manuscript.

FUNDING

REFERENCES

Anderegg, W. R., Trugman, A. T., Badgley, G., Konings, A. G., and Shaw, J. (2020). Divergent forest sensitivity to repeated extreme droughts. *Nat. Clim. Chang.* 10, 1091–1095. doi: 10.1038/s41558-020-00919-1

Ayub, G., Smith, R. A., Tissue, D. T., and Atkin, O. K. (2011). Impacts of drought on leaf respiration in darkness and light in *Eucalyptus saligna* exposed to industrial-age atmospheric CO2 and growth temperature. *New Phytol.* 190, 1003–1018. doi: 10.1111/j.1469-8137.2011.03673.x

Blackman, C. J., Brodribb, T. J., and Jordan, G. J. (2009). Leaf hydraulics and drought stress: response, recovery and survivorship in four woody temperate plant species. *Plant Cell Environ.* 32, 1584–1595. doi: 10.1111/j.1365-3040.2009.02023.x

Brodribb, T., and Holbrook, N. M. (2004). Diurnal depression of leaf hydraulic conductance in a tropical tree species. *Plant Cell Environ.* 27, 820–827. doi: 10.1111/j.1365-3040.2004.01188.x

Brodribb, T. J., and Cochard, H. (2009). Hydraulic failure defines the recovery and point of death in water-stressed conifers. *Plant Physiol.* 149, 575–584. doi: 10.1104/pp.108.129783

Brodribb, T. J., and Holbrook, N. M. (2003). Stomatal closure during leaf dehydration, correlation with other leaf physiological traits. *Plant Physiol.* 132, 2166–2173. doi: 10.1104/pp.103.023879

Brodribb, T. J., Powers, J., Cochard, H., and Choat, B. (2020). Hanging by a thread? Forests and drought. *Science* 368, 261–266.

Butcher, P., McDonald, M., and Bell, J. (2009). Congruence between environmental parameters, morphology and genetic structure in Australia's most widely distributed eucalypt, *Eucalyptus camaldulensis. Tree Genet. Genomes* 5, 189–210. doi: 10.1007/s11295-008-0169-6

Carmo-Silva, A. E., Keys, A. J., Andralojc, P. J., Powers, S. J., Arrabaça, M. C., and Parry, M. A. (2010). Rubisco activities, properties, and regulation in three different C4 grasses under drought. *J. Exp. Bot.* 61, 2355–2366. doi: 10.1093/jxb/erq071

Chapin, F. S. III, Schulze, E., and Mooney, H. A. (1990). The ecology and economics of storage in plants. *Annu. Rev. Ecol. Evol. Syst.* 21, 423–447. doi: 10.1146/annurev.es.21.110190.002231

Choat, B., Brodribb, T. J., Brodersen, C. R., Duursma, R. A., Lopez, R., and Medlyn, B. E. (2018). Triggers of tree mortality under drought. *Nature* 558, 531–539. doi: 10.1038/s41586-018-0240-x

Chuste, P. A., Maillard, P., Bréda, N., Levillain, J., Thirion, E., Wortemann, R., et al. (2020). Sacrificing growth and maintaining a dynamic carbohydrate storage are key processes for promoting beech survival under prolonged drought conditions. *Trees* 34, 381–394. doi: 10.1007/s00468-019-01923-5

Dai, A. (2013). Increasing drought under global warming in observations and models. *Nat. Clim. Chang.* 3, 52–58. doi: 10.1038/nclimate1633

De Baerdemaeker, N. J., Salomón, R. L., De Roo, L., and Steppe, K. (2017). Sugars from woody tissue photosynthesis reduce xylem vulnerability to cavitation. *New Phytol.* 216, 720–727. doi: 10.1111/nph.14787

Doody, T. M., Colloff, M. J., Davies, M., Koul, V., Benyon, R. G., and Nagler, P. L. (2015). Quantifying water requirements of riparian river red gum (*Eucalyptus camaldulensis*) in the Murray-Darling Basin, Australia-implications for the management of environmental flows. *Ecohydrology* 8, 1471–1487. doi: 10.1002/eco.1598

Duan, H., Amthor, J. S., Duursma, R. A., O'grady, A. P., Choat, B., and Tissue, D. T. (2013). Carbon dynamics of eucalypt seedlings exposed to progressive drought in elevated [CO2] and elevated temperature. *Tree Physiol.* 33, 779–792. doi: 10.1093/treephys/tpt061

Duursma, R. A. (2015). Plantecophys-an R package for analysing and modelling leaf gas exchange data. *PLoS One* 10:e0143346. doi: 10.1371/journal.pone.0143346

Flexas, J., Barón, M., Bota, J., Ducruet, J. M., Gallé, A., Galmés, J., et al. (2009). Photosynthesis limitations during water stress acclimation and recovery in the drought-adapted Vitis hybrid Richter-110 (V. berlandieri× V. rupestris). *J. Exp. Bot.* 60, 2361–2377. doi: 10.1093/jxb/erp069

Flexas, J., Bota, J., Galmes, J., Medrano, H., and Ribas-Carbó, M. (2006a). Keeping a positive carbon balance under adverse conditions: responses of photosynthesis and respiration to water stress. *Physiol. Plant* 127, 343–352. doi: 10.1111/j.1399-3054.2006.00621.x

Flexas, J., Bota, J., Loreto, F., Cornic, G., and Sharkey, T. (2004). Diffusive and metabolic limitations to photosynthesis under drought and salinity in C3 plants. *Plant Biol.* 6, 269–279. doi: 10.1055/s-2004-820867

Flexas, J., Galmes, J., Ribas-Carbo, M., and Medrano, H. (2005). "The effects of water stress on plant respiration," in *Plant Respiration*, eds H. Lambers and M. Ribas-Carbo (Dordrecht: Springer), doi: 10.1007/1-4020-3589-6_6

Flexas, J., Ribas-Carbó, M., Bota, J., Galmés, J., Henkle, M., Martínez-Cañellas, S., et al. (2006b). Decreased Rubisco activity during water stress is not induced by decreased relative water content but related to conditions of low stomatal conductance and chloroplast CO2 concentration. *New Phytol.* 172, 73–82. doi: 10.1111/j.1469-8137.2006.01794.x

Flexas, J., Ribas-Carbo, M., Diaz-Espejo, A., Galmes, J., and Medrano, H. (2008). Mesophyll conductance to CO2: current knowledge and future prospects. *Plant Cell Environ.* 31, 602–621. doi: 10.1111/j.1365-3040.2007.01757.x

Galmés, J., Aranjuelo, I., Medrano, H., and Flexas, J. (2013). Variation in Rubisco content and activity under variable climatic factors. *Photosynth. Res.* 117, 73–90. doi: 10.1007/s11120-013-9861-y

Galmés, J., Flexas, J., Savé, R., and Medrano, H. (2007). Water relations and stomatal characteristics of Mediterranean plants with different growth forms and leaf habits: responses to water stress and recovery. *Plant Soil* 290, 139–155. doi: 10.1007/s11104-006-9148-6

Gessler, A., Bottero, A., Marshall, J., and Arend, M. (2020). The way back: recovery of trees from drought and its implication for acclimation. *New Phytol.* 228, 1704–1709. doi: 10.1111/nph.16703

Granda, E., and Camarero, J. J. (2017). Drought reduces growth and stimulates sugar accumulation: new evidence of environmentally driven non-structural carbohydrate use. *Tree Physiol.* 37, 997–1000. doi: 10.1093/treephys/tpx097

Grassi, G., and Magnani, F. (2005). Stomatal, mesophyll conductance and biochemical limitations to photosynthesis as affected by drought and leaf ontogeny in ash and oak trees. *Plant Cell Environ.* 28, 834–849. doi: 10.1111/j.1365-3040.2005.01333.x

Hagedorn, F., Joseph, J., Peter, M., Luster, J., Pritsch, K., Geppert, U., et al. (2016). Recovery of trees from drought depends on belowground sink control. *Nat. Plants* 2:16111. doi: 10.1038/nplants.2016.111

He, W., Liu, H., Qi, Y., Liu, F., and Zhu, X. (2020). Patterns in nonstructural carbohydrate contents at the tree organ level in response to drought duration. *Glob. Chang. Biol.* 26, 3627–3638. doi: 10.1111/gcb.15078

Joseph, J., Gao, D., Backes, B., Bloch, C., Brunner, I., Gleixner, G., et al. (2020). Rhizosphere activity in an old-growth forest reacts rapidly to changes in soil moisture and shapes whole-tree carbon allocation. *Proc. Natl. Acad. Sci. U.S.A.* 117, 24885–24892. doi: 10.1073/pnas.2014084117

Kannenberg, S. A., Schwalm, C. R., and Anderegg, W. R. (2020). Ghosts of the past: how drought legacy effects shape forest functioning and carbon cycling. *Ecol. Lett.* 23, 891–901. doi: 10.1111/ele.13485

Kitao, M., Lei, T. T., Koike, T., Tobita, H., and Maruyama, Y. (2003). Higher electron transport rate observed at low intercellular CO2 concentration in long-term drought-acclimated leaves of Japanese mountain birch (*Betula ermanii*). *Physiol. Plant* 118, 406–413. doi: 10.1034/j.1399-3054.2003.00120.x

Klein, T., Hoch, G., Yakir, D., and Körner, C. (2014). Drought stress, growth and nonstructural carbohydrate dynamics of pine trees in a semi-arid forest. *Tree Physiol.* 34, 981–992. doi: 10.1093/treephys/tpu071

Körner, C. (2015). Paradigm shift in plant growth control. *Curr. Opin. Plant Biol.* 25, 107–114. doi: 10.1016/j.pbi.2015.05.003

Li, X., Piao, S., Wang, K., Wang, X., Wang, T., Ciais, P., et al. (2020). Temporal trade-off between gymnosperm resistance and resilience increases forest sensitivity to extreme drought. *Nat. Ecol. Evol.* 4, 1075–1083. doi: 10.1038/s41559-020-1217-3

Martínez-Vilalta, J., Sala, A., Asensio, D., Galiano, L., Hoch, G., Palacio, S., et al. (2016). Dynamics of non-structural carbohydrates in terrestrial plants: a global synthesis. *Ecol. Monogr.* 86, 495–516. doi: 10.1002/ecm.1231

Menezes-Silva, P. E., Sanglard, L. M., Ávila, R. T., Morais, L. E., Martins, S. C., Nobres, P., et al. (2017). Photosynthetic and metabolic acclimation to repeated drought events play key roles in drought tolerance in coffee. *J. Exp. Bot.* 68, 4309–4322. doi: 10.1093/jxb/erx211

Mitchell, P. J., O'Grady, A. P., Tissue, D. T., White, D. A., Ottenschlaeger, M. L., and Pinkard, E. A. (2013). Drought response strategies define the relative contributions of hydraulic dysfunction and carbohydrate depletion during tree mortality. *New Phytol.* 197, 862–872. doi: 10.1111/nph.12064

O'Brien, M. J., Engelbrecht, B. M., Joswig, J., Pereyra, G., Schuldt, B., Jansen, S., et al. (2017a). A synthesis of tree functional traits related to drought-induced mortality in forests across climatic zones. *J. Appl. Ecol.* 54, 1669–1686. doi: 10.1111/1365-2664.12874

O'Brien, M. J., Ong, R., and Reynolds, G. (2017b). Intra-annual plasticity of growth mediates drought resilience over multiple years in tropical seedling communities. *Glob. Chang. Biol.* 23, 4235–4244. doi: 10.1111/gcb.13658

Ouyang, S. N., Gessler, A., Saurer, M., Hagedorn, F., Gao, D. C., Wang, X. Y., et al. (2021). Root carbon and nutrient homeostasis determines downy oak sapling survival and recovery from drought. *Tree Physiol.* 41, 1400–1412. doi: 10.1093/treephys/tpab019

Parry, M. A., Andralojc, P. J., Khan, S., Lea, P. J., and Keys, A. J. (2002). Rubisco activity: effects of drought stress. *Ann. Bot.* 89, 833–839. doi: 10.1093/aob/mcf103

Piper, F. I., Fajardo, A., and Hoch, G. (2017). Single-provenance mature conifers show higher non-structural carbohydrate storage and reduced growth in a drier location. *Tree Physiol.* 37, 1001–1010. doi: 10.1093/treephys/tpx061

R Core Team (2013). *R: A Language and Environment for Statistical Computing.* Vienna: R Foundation for Statistical Computing. Available online at: http://www.R-project.org/

Ruehr, N. K., Grote, R., Mayr, S., and Arneth, A. (2019). Beyond the extreme: recovery of carbon and water relations in woody plants following heat and drought stress. *Tree Physiol.* 39, 1285–1299. doi: 10.1093/treephys/tpz032

Sala, A., and Hoch, G. (2009). Height-related growth declines in ponderosa pine are not due to carbon limitation. *Plant Cell Environ.* 32, 22–30. doi: 10.1111/j.1365-3040.2008.01896.x

Sala, A., Woodruff, D. R., and Meinzer, F. C. (2012). Carbon dynamics in trees: feast or famine? *Tree Physiol.* 32, 764–775. doi: 10.1093/treephys/tpr143

Schmitt, A., Trouvé, R., Seynave, I., and Lebourgeois, F. (2020). Decreasing stand density favors resistance, resilience, and recovery of *Quercus petraea* trees to a severe drought, particularly on dry sites. *Ann. For. Sci.* 77, 1–21. doi: 10.1007/s13595-020-00959-9

Signori-Müller, C., Oliveira, R. S., de Vasconcellos Barros, F., Tavares, J. V., Gilpin, M., Diniz, F. C., et al. (2021). Non-structural carbohydrates mediate seasonal water stress across Amazon forests. *Nat. Commun.* 12, 1–9. doi: 10.1038/s41467-021-22378-8

Skelton, R. P., Brodribb, T. J., McAdam, S. A., and Mitchell, P. J. (2017). Gas exchange recovery following natural drought is rapid unless limited by loss of leaf hydraulic conductance: evidence from an evergreen woodland. *New Phytol.* 215, 1399–1412. doi: 10.1111/nph.14652

Stuart-Haëntjens, E., De Boeck, H. J., Lemoine, N. P., Mänd, P., Kröel-Dulay, G., Schmidt, I. K., et al. (2018). Mean annual precipitation predicts primary production resistance and resilience to extreme drought. *Sci. Total Environ.* 636, 360–366. doi: 10.1016/j.scitotenv.2018.04.290

Tomasella, M., Petrussa, E., Petruzzellis, F., Nardini, A., and Casolo, V. (2020). The possible role of non-structural carbohydrates in the regulation of tree hydraulics. *Int. J. Mol. Sci.* 21:144. doi: 10.3390/ijms21010144

Trifilò, P., Casolo, V., Raimondo, F., Petrussa, E., Boscutti, F., Gullo, M. A. L., et al. (2017). Effects of prolonged drought on stem non-structural carbohydrates content and post-drought hydraulic recovery in *Laurus nobilis* L.: the possible link between carbon starvation and hydraulic failure. *Plant Physiol. Biochem.* 120, 232–241. doi: 10.1016/j.plaphy.2017.10.003

Wu, X., Liu, H., Li, X., Ciais, P., Babst, F., Guo, W., et al. (2018). Differentiating drought legacy effects on vegetation growth over the temperate Northern Hemisphere. *Glob. Chang. Biol.* 24, 504–516. doi: 10.1111/gcb.13920

Xu, Z., Zhou, G., and Shimizu, H. (2010). Plant responses to drought and rewatering. *Plant Signal Behav.* 5, 649–654. doi: 10.4161/psb.5.6.11398

Zait, Y., Shtein, I., and Schwartz, A. (2019). Long-term acclimation to drought, salinity and temperature in the thermophilic tree *Ziziphus spina-christi*: revealing different tradeoffs between mesophyll and stomatal conductance. *Tree Physiol.* 39, 701–716. doi: 10.1093/treephys/tpy133

Zhou, S., Medlyn, B., Sabaté, S., Sperlich, D., and Prentice, I. C. (2014). Short-term water stress impacts on stomatal, mesophyll and biochemical limitations to photosynthesis differ consistently among tree species from contrasting climates. *Tree Physiol.* 34, 1035–1046. doi: 10.1093/treephys/tpu072